

Science Newsletter

2023 Volume 10 (Total 46) Website:
<http://lib.jsut.edu.cn/2018/1015/c5474a113860/page.htm>, December 2023

Contents

INTRODUCTION:	2
I TOPICS	2
APPLIED MECHANICS	2
AUTOMATION	5
BIOMECHANICS	10
COMPUTATIONAL FLUID DYNAMICS	12
DESIGN AND MANUFACTURING	17
II CONCENTRATION	21
PHYSICS	21
MATERIALS	22
CHEMISTRY	24
BIOLOGY	25
III CALLING FOR PAPERS	28
ACAE 2024	28
ICMENS 2024	30
ICMES 2024	32
ICAMM--SCOPUS 2024	33


Introduction:

There are 3 main elements in the Science Newsletter is composed. In the first part, we provide articles about central issues for each discipline in this university, and they are provided with one subject for a time. In the second part, we select articles from the top journals in the whole science research. In the third part, we post information about calling papers for international conferences. Hopefully, some of the information in this manuscript may be useful for those who are dedicating to scientific career. Besides, the journals are also posted on the website of our library, and they are available to be accessed any time at <http://lib.jsut.edu.cn/2018/1015/c5474a113860/page.htm>. If there are any questions or suggestions, please send e-mails to 289595883@qq.com in no hesitate.

I Topics

The key word of this month is **Mechanical Engineering**. We list several articles which are related to the top concerned topics of computer science researches. The articles are classified in 5 categories, and they are: **Applied Mechanics, Automation, Biomechanics, Computational Fluid Dynamics** and **Design and Manufacturing**. Also, the listed articles are all arranged in a descending sort of impact factor in order to make it convenient to read. There are also links to both official site and full text for each article.

APPLIED MECHANICS

Lancet (impact factor: 168.94) 1 

Estimating the cause-specific relative risks of non-optimal temperature on daily mortality: a two-part modelling approach applied to the Global Burden of Disease Study

Katrin G Burkart · Michael Brauer · Aleksandr Y Aravkin et al

Background

Associations between high and low temperatures and increases in mortality and morbidity have been previously reported, yet no comprehensive assessment of disease burden has been done. Therefore, we aimed to estimate the global and regional burden

due to non-optimal temperature exposure.

Methods

In part 1 of this study, we linked deaths to daily temperature estimates from the ERA5 reanalysis dataset. We modelled the cause-specific relative risks for 176 individual causes of death along daily temperature and 23 mean temperature zones using a two-dimensional spline within a Bayesian meta-regression framework. We then calculated the cause-specific and total temperature-attributable burden for the countries for which daily mortality data were available. In part 2, we applied cause-specific relative risks from part 1 to all locations globally. We combined exposure–response curves with daily gridded temperature and calculated the cause-specific burden based on the underlying burden of disease from the Global Burden of Diseases, Injuries, and Risk Factors Study, for the years 1990–2019. Uncertainty from all components of the modelling chain, including risks, temperature exposure, and theoretical minimum risk exposure levels, defined as the temperature of minimum mortality across all included causes, was propagated using posterior simulation of 1000 draws.


Findings

We included 64·9 million individual International Classification of Diseases-coded deaths from nine different countries, occurring between Jan 1, 1980, and Dec 31, 2016. 17 causes of death met the inclusion criteria. Ischaemic heart disease, stroke, cardiomyopathy and myocarditis, hypertensive heart disease, diabetes, chronic kidney disease, lower respiratory infection, and chronic obstructive pulmonary disease showed J-shaped relationships with daily temperature, whereas the risk of external causes (eg, homicide, suicide, drowning, and related to disasters, mechanical, transport, and other unintentional injuries) increased monotonically with temperature. The theoretical minimum risk exposure levels varied by location and year as a function of the underlying cause of death composition. Estimates for non-optimal temperature ranged from 7·98 deaths (95% uncertainty interval 7·10–8·85) per 100 000 and a population attributable fraction (PAF) of 1·2% (1·1–1·4) in Brazil to 35·1 deaths (29·9–40·3) per 100 000 and a PAF of 4·7% (4·3–5·1) in China. In 2019, the average cold-attributable mortality exceeded heat-attributable mortality in all countries for which data were available. Cold effects were most pronounced in China with PAFs of 4·3% (3·9–4·7) and attributable rates of 32·0 deaths (27·2–36·8) per 100 000 and in New Zealand with 3·4% (2·9–3·9) and 26·4 deaths (22·1–30·2). Heat effects were most pronounced in China with PAFs of 0·4% (0·3–0·6) and attributable rates of 3·25 deaths (2·39–4·24) per 100 000 and in Brazil with 0·4% (0·3–0·5) and 2·71 deaths (2·15–3·37). When applying our framework to all countries globally, we estimated that 1·69 million (1·52–1·83) deaths were attributable to non-optimal temperature globally in 2019. The highest heat-attributable burdens were observed in south and southeast Asia, sub-Saharan Africa, and North Africa and the Middle East, and the highest cold-attributable burdens in eastern and central Europe, and central Asia.

Interpretation

Acute heat and cold exposure can increase or decrease the risk of mortality for a diverse set of causes of death. Although in most regions cold effects dominate, locations with high prevailing temperatures can exhibit substantial heat effects far exceeding cold-

attributable burden. Particularly, a high burden of external causes of death contributed to strong heat impacts, but cardiorespiratory diseases and metabolic diseases could also be substantial contributors. Changes in both exposures and the composition of causes of death drove changes in risk over time. Steady increases in exposure to the risk of high temperature are of increasing concern for health.


ACM Computing Surveys (impact factor: 16.62) 1 

Challenges and Opportunities for Practical and Effective Dynamic Information Flow Tracking

Christopher Brant · Prakash Shrestha · Benjamin Mixon-Baca et.al

Abstract:

Information flow tracking was proposed more than 40 years ago to address the limitations of access control mechanisms to guarantee the confidentiality and integrity of information flowing within a system, but has not yet been widely applied in practice for security solutions. Here, we survey and systematize literature on dynamic information flow tracking (DIFT) to discover challenges and opportunities to make it practical and effective for security solutions. We focus on common knowledge in the literature and lingering research gaps from two dimensions— (i) the layer of abstraction where DIFT is implemented (software, software/hardware, or hardware) and (ii) the security goal (confidentiality and/or integrity). We observe that two major limitations hinder the practical application of DIFT for on-the-fly security applications: (i) high implementation overhead and (ii) incomplete information flow tracking (low accuracy). We posit, after review of the literature, that addressing these major impedances via hardware parallelism can potentially unleash DIFT’s great potential for systems security, as it can allow security policies to be implemented in a built-in and standardized fashion. Furthermore, we provide recommendations for the next generation of practical and efficient DIFT systems with an eye towards hardware-supported implementations.

Nature Reviews Gastroenterology & Hepatology (impact factor: 65.11) 1 


Advances in immunotherapy for hepatocellular carcinoma

Bruno Sangro · Pablo Sarobe · Sandra Hervás-Stubbs, et.al

Abstract:

Hepatocellular carcinoma (HCC) is a prevalent disease with a progression that is modulated by the immune system. Systemic therapy is used in the advanced stage and until 2017 consisted only of antiangiogenic tyrosine kinase inhibitors (TKIs). Immunotherapy with checkpoint inhibitors has shown strong anti-tumour activity in a subset of patients and the combination of the anti-PDL1 antibody atezolizumab and the VEGF-neutralizing antibody bevacizumab has or will soon become the standard

of care as a first-line therapy for HCC, whereas the anti-PD1 agents nivolumab and pembrolizumab are used after TKIs in several regions. Other immune strategies such as adoptive T-cell transfer, vaccination or virotherapy have not yet demonstrated consistent clinical activity. Major unmet challenges in HCC checkpoint immunotherapy are the discovery and validation of predictive biomarkers, advancing treatment to earlier stages of the disease, applying the treatment to patients with liver dysfunction and the discovery of more effective combinatorial or sequential approaches. Combinations with other systemic or local treatments are perceived as the most promising opportunities in HCC and some are already under evaluation in large-scale clinical trials. This Review provides up-to-date information on the best use of currently available immunotherapies in HCC and the therapeutic strategies under development.

Nature Energy (impact factor: 56.73) 1 


Reactive boride infusion stabilizes Ni-rich cathodes for lithium-ion batteries

Moonsu Yoon · Yanhao Dong · Jaeseong Hwang, et.al

Abstract:

Engineered polycrystalline electrodes are critical to the cycling stability and safety of lithium-ion batteries, yet it is challenging to construct high-quality coatings at both the primary- and secondary-particle levels. Here we present a room-temperature synthesis route to achieve a full surface coverage of secondary particles and facile infusion into grain boundaries, and thus offer a complete ‘coating-plus-infusion’ strategy. Cobalt boride metallic glass was successfully applied to a Ni-rich layered cathode $\text{LiNi}_{0.8}\text{Co}_{0.1}\text{Mn}_{0.1}\text{O}_2$. It dramatically improved the rate capability and cycling stability, including under high-discharge-rate and elevated-temperature conditions and in pouch full-cells. The superior performance originates from a simultaneous suppression of the microstructural degradation of the intergranular cracking and of side reactions with the electrolyte. Atomistic simulations identified the critical role of strong selective interfacial bonding, which offers not only a large chemical driving force to ensure uniform reactive wetting and facile infusion, but also lowers the surface/interface oxygen activity, which contributes to the exceptional mechanical and electrochemical stabilities of the infused electrode.

Automation

Lancet (impact factor: 168.94) 1 

A comparison of two hybrid closed-loop systems in adolescents and young adults with type 1 diabetes (FLAIR): a multicentre, randomised, crossover trial

Background

Management of type 1 diabetes is challenging. We compared outcomes using a commercially available hybrid closed-loop system versus a new investigational system with features potentially useful for adolescents and young adults with type 1 diabetes.

Methods

In this multinational, randomised, crossover trial (Fuzzy Logic Automated Insulin Regulation [FLAIR]), individuals aged 14–29 years old, with a clinical diagnosis of type 1 diabetes with a duration of at least 1 year, using either an insulin pump or multiple daily insulin injections, and glycated haemoglobin (HbA1c) levels of 7.0–11.0% (53–97 mmol/mol) were recruited from seven academic-based endocrinology practices, four in the USA, and one each in Germany, Israel, and Slovenia. After a run-in period to teach participants how to use the study pump and continuous glucose monitor, participants were randomly assigned (1:1) using a computer-generated sequence, with a permuted block design (block sizes of two and four), stratified by baseline HbA1c and use of a personal MiniMed 670G system (Medtronic) at enrolment, to either use of a MiniMed 670G hybrid closed-loop system (670G) or the investigational advanced hybrid closed-loop system (Medtronic) for the first 12-week period, and then participants were crossed over with no washout period, to the other group for use for another 12 weeks. Masking was not possible due to the nature of the systems used. The coprimary outcomes, measured with continuous glucose monitoring, were proportion of time that glucose levels were above 180 mg/dL (>10.0 mmol/L) during 0600 h to 2359 h (ie, daytime), tested for superiority, and proportion of time that glucose levels were below 54 mg/dL (<3.0 mmol/L) calculated over a full 24-h period, tested for non-inferiority (non-inferiority margin 2%). Analysis was by intention to treat. Safety was assessed in all participants randomly assigned to treatment. This trial is registered with ClinicalTrials.gov, NCT03040414, and is now complete.


Findings

Between June 3 and Aug 22, 2019, 113 individuals were enrolled into the trial. Mean age was 19 years (SD 4) and 70 (62%) of 113 participants were female. Mean proportion of time with daytime glucose levels above 180 mg/dL (>10.0 mmol/L) was 42% (SD 13) at baseline, 37% (9) during use of the 670G system, and 34% (9) during use of the advanced hybrid closed-loop system (mean difference [advanced hybrid closed-loop system minus 670G system] –3.00% [95% CI –3.97 to –2.04]; $p < 0.0001$). Mean 24-h proportion of time with glucose levels below 54 mg/dL (<3.0 mmol/L) was 0.46% (SD 0.42) at baseline, 0.50% (0.35) during use of the 670G system, and 0.46% (0.33) during use of the advanced hybrid closed-loop system (mean difference [advanced hybrid closed-loop system minus 670G system] –0.06% [95% CI –0.11 to –0.02]; $p < 0.0001$ for non-inferiority). One severe hypoglycaemic event occurred in the advanced hybrid closed-loop system group, determined to be unrelated to study treatment, and none occurred in the 670G group.

Interpretation

Hyperglycaemia was reduced without increasing hypoglycaemia in adolescents and young adults with type 1 diabetes using the investigational advanced hybrid closed-loop system compared with the commercially available MiniMed 670G system. Testing an advanced hybrid closed-loop system in populations that are underserved due to socioeconomic factors and testing during pregnancy and in individuals with impaired awareness of hypoglycaemia would advance the effective use of

this technology.

Lancet Respiratory Medicine (impact factor: 76.22) 1 

Colchicine for community-treated patients with COVID-19 (COLCORONA): a phase 3, randomised, double-blinded, adaptive, placebo-controlled, multicentre trial

Jean-Claude Tardif · Nadia Bouabdallaoui · Philippe L L'Allier et. al

Abstract:

Background

Evidence suggests a role for excessive inflammation in COVID-19 complications. Colchicine is an oral anti-inflammatory medication beneficial in gout, pericarditis, and coronary disease. We aimed to investigate the effect of colchicine on the composite of COVID-19-related death or hospital admission.

Methods

The present study is a phase 3, randomised, double-blind, adaptive, placebo-controlled, multicentre trial. The study was done in Brazil, Canada, Greece, South Africa, Spain, and the USA, and was led by the Montreal Heart Institute. Patients with COVID-19 diagnosed by PCR testing or clinical criteria who were not being treated in hospital were eligible if they were at least 40 years old and had at least one high-risk characteristic. The randomisation list was computer-generated by an unmasked biostatistician, and masked randomisation was centralised and done electronically through an automated interactive web-response system. The allocation sequence was unstratified and used a 1:1 ratio with a blocking schema and block sizes of six. Patients were randomly assigned to receive orally administered colchicine (0.5 mg twice per day for 3 days and then once per day for 27 days thereafter) or matching placebo. The primary efficacy endpoint was the composite of death or hospital admission for COVID-19. Vital status at the end of the study was available for 97.9% of patients. The analyses were done according to the intention-to-treat principle. The COLCORONA trial is registered with ClinicalTrials.gov (NCT04322682) and is now closed to new participants.


Findings

Trial enrolment began in March 23, 2020, and was completed in Dec 22, 2020. A total of 4488 patients (53.9% women; median age 54.0 years, IQR 47.0–61.0) were enrolled and 2235 patients were randomly assigned to colchicine and 2253 to placebo. The primary endpoint occurred in 104 (4.7%) of 2235 patients in the colchicine group and 131 (5.8%) of 2253 patients in the placebo group (odds ratio [OR] 0.79, 95.1% CI 0.61–1.03; $p=0.081$). Among the 4159 patients with PCR-confirmed COVID-19, the primary endpoint occurred in 96 (4.6%) of 2075 patients in the colchicine group and 126 (6.0%) of 2084 patients in the placebo group (OR 0.75, 0.57–0.99; $p=0.042$). Serious adverse events were reported in 108 (4.9%) of 2195 patients in the colchicine group and 139 (6.3%) of 2217 patients in the placebo group ($p=0.051$); pneumonia occurred in 63 (2.9%) of 2195 patients in the colchicine group and 92 (4.1%) of 2217 patients in the placebo group ($p=0.021$). Diarrhoea was reported in 300 (13.7%) of 2195 patients in the colchicine group and 161 (7.3%) of 2217 patients

in the placebo group ($p < 0.0001$).

Interpretation

In community-treated patients including those without a mandatory diagnostic test, the effect of colchicine on COVID-19-related clinical events was not statistically significant. Among patients with PCR-confirmed COVID-19, colchicine led to a lower rate of the composite of death or hospital admission than placebo. Given the absence of orally administered therapies to prevent COVID-19 complications in community-treated patients and the benefit of colchicine in patients with PCR-proven COVID-19, this safe and inexpensive anti-inflammatory agent could be considered for use in those at risk of complications. Notwithstanding these considerations, replication in other studies of PCR-positive community-treated patients is recommended.

New England Journal of Medicine (impact factor: 158.52) 1 

100,000 Genomes Pilot on Rare-Disease Diagnosis in Health Care — Preliminary Report

Damian Smedley · Katherine R Smith · Antonio Rueda Martin et.al

Abstract:

BACKGROUND

The U.K. 100,000 Genomes Project is in the process of investigating the role of genome sequencing in patients with undiagnosed rare diseases after usual care and the alignment of this research with health care implementation in the U.K. National Health Service. Other parts of this project focus on patients with cancer and infection.

METHODS

We conducted a pilot study involving 4660 participants from 2183 families, among whom 161 disorders covering a broad spectrum of rare diseases were present. We collected data on clinical features with the use of Human Phenotype Ontology terms, undertook genome sequencing, applied automated variant prioritization on the basis of applied virtual gene panels and phenotypes, and identified novel pathogenic variants through research analysis.


RESULTS

Diagnostic yields varied among family structures and were highest in family trios (both parents and a proband) and families with larger pedigrees. Diagnostic yields were much higher for disorders likely to have a monogenic cause (35%) than for disorders likely to have a complex cause (11%). Diagnostic yields for intellectual disability, hearing disorders, and vision disorders ranged from 40 to 55%. We made genetic diagnoses in 25% of the probands. A total of 14% of the diagnoses were made by means of the combination of research and automated approaches, which was critical for cases in which we found etiologic noncoding, structural, and mitochondrial genome variants and coding variants poorly covered by exome sequencing. Cohortwide burden testing across 57,000 genomes enabled the discovery of three new

disease genes and 19 new associations. Of the genetic diagnoses that we made, 25% had immediate ramifications for clinical decision making for the patients or their relatives.

CONCLUSIONS

Our pilot study of genome sequencing in a national health care system showed an increase in diagnostic yield across a range of rare diseases. (Funded by the National Institute for Health Research and others.)

Lancet (impact factor: 168.94) 1 

Gestational age recorded at delivery versus estimations using antenatal care data from the Electronic Maternal and Child Health Registry in the West Bank: a comparative analysis

Mervett Isbeih · Mahima Venkateswaran · Eatimad Abbas, et. al

Abstract:

Background

Estimated dates of delivery have important consequences for clinical decisions during pregnancy and labour. The Electronic Maternal and Child Health Registry (MCH eRegistry) in Palestine includes antenatal care data and birth data from hospitals. Our objective was to compare computed best estimates of gestational age in the MCH eRegistry with the gestational ages recorded by health-care providers in hospital delivery units.

Methods

We obtained data for pregnant women in the West Bank registered in the MCH eRegistry from Jan 1, 2017 to March 31, 2017. Best estimates of gestational age in the registry are automated and based on a standard pregnancy duration of 280 days and ultrasound-based pregnancy dating before 20 weeks' gestation or the woman's last menstrual period date. Hospital recorded gestational ages are reported by care providers in delivery units and are rounded to the nearest week. We calculated proportions of gestational ages (with 95% CIs) from both sources that fell into the categories of term, very preterm (24–32 weeks' gestation), preterm (33–37 weeks), or post-term (>42 weeks).

Findings

1924 women were included in the study. The median hospital recorded gestational age was 39 weeks (IQR 38–40 weeks) and according to MCH eRegistry estimates was 39 weeks and 5 days (IQR 38 weeks and 1 day to 40 weeks and 5 days). Proportions of very preterm, preterm, and post-term deliveries were higher based on MCH eRegistry estimates than on hospital recorded gestational ages (very preterm 3%, 95% CI 2–4 vs 2%, 1–2; preterm 6%, 5–7 vs 5%, 3–6 ; post-term 6%, 5–7 vs 1%, 1–2).

Interpretation

In addition to clinical care, the proportions of term, very preterm, preterm, and post-term births can have implications for public health monitoring. The proportion of

deliveries within the normal range of term gestation was calculated to be higher by care providers in delivery units than by MCH eRegistry estimates. Extending the access of hospitals to information from antenatal care in the MCH e-Registry could improve continuity of data and better care for pregnant women.

BIOMECHANICS

Nature Reviews Cancer (impact factor: 78.53) 1 ☒

The matrix in cancer

Thomas R. Cox

Abstract:

The extracellular matrix is a fundamental, core component of all tissues and organs, and is essential for the existence of multicellular organisms. From the earliest stages of organism development until death, it regulates and fine-tunes every cellular process in the body. In cancer, the extracellular matrix is altered at the biochemical, biomechanical, architectural and topographical levels, and recent years have seen an exponential increase in the study and recognition of the importance of the matrix in solid tumours. Coupled with the advancement of new technologies to study various elements of the matrix and cell–matrix interactions, we are also beginning to see the deployment of matrix-centric, stromal targeting cancer therapies. This Review touches on many of the facets of matrix biology in solid cancers, including breast, pancreatic and lung cancer, with the aim of highlighting some of the emerging interactions of the matrix and influences that the matrix has on tumour onset, progression and metastatic dissemination, before summarizing the ongoing work in the field aimed at developing therapies to co-target the matrix in cancer and cancer metastasis.

Science (impact factor: 56.91) 1 ☒

Fossil apes and human evolution

Sergio Almécija · Ashley S. Hammond · Nathan E et.al

Abstract:

Humans diverged from apes (chimpanzees, specifically) toward the end of the Miocene ~9.3 million to 6.5 million years ago. Understanding the origins of the human lineage (hominins) requires reconstructing the morphology, behavior, and environment of the chimpanzee-human last common ancestor. Modern hominoids (that is, humans and apes) share multiple features (for example, an orthograde body plan facilitating upright positional behaviors). However, the fossil record indicates that living hominoids constitute narrow representatives of an ancient radiation of

more widely distributed, diverse species, none of which exhibit the entire suite of locomotor adaptations present in the extant relatives. Hence, some modern ape similarities might have evolved in parallel in response to similar selection pressures. Current evidence suggests that hominins originated in Africa from Miocene ape ancestors unlike any living species.

Nature Reviews Cancer (impact factor: 78.53) 1 ☒

Decoding leader cells in collective cancer invasion

Samuel A. Vilchez Mercedes · Federico Bocci · Herbert Levine et.al

Abstract:

Collective cancer invasion with leader–follower organization is increasingly recognized as a predominant mechanism in the metastatic cascade. Leader cells support cancer invasion by creating invasion tracks, sensing environmental cues and coordinating with follower cells biochemically and biomechanically. With the latest developments in experimental and computational models and analysis techniques, the range of specific traits and features of leader cells reported in the literature is rapidly expanding. Yet, despite their importance, there is no consensus on how leader cells arise or their essential characteristics. In this Perspective, we propose a framework for defining the essential aspects of leader cells and provide a unifying perspective on the varying cellular and molecular programmes that are adopted by each leader cell subtype to accomplish their functions. This Perspective can lead to more effective strategies to interdict a major contributor to metastatic capability.

Science (impact factor: 56.91) 1 ☒


Acrobatic squirrels learn to leap and land on tree branches without falling

Nathaniel H Hunt · Judy Jinn · Lucia F Jacobs, et.al

Abstract

Arboreal animals often leap through complex canopies to travel and avoid predators. Their success at making split-second, potentially life-threatening decisions of biomechanical capability depends on their skillful use of acrobatic maneuvers and learning from past efforts. Here, we found that free-ranging fox squirrels (*Sciurus niger*) leaping across unfamiliar, simulated branches decided where to launch by balancing a trade-off between gap distance and branch-bending compliance. Squirrels quickly learned to modify impulse generation upon repeated leaps from unfamiliar, compliant beams. A repertoire of agile landing maneuvers enabled targeted leaping without falling. Unanticipated adaptive landing and leaping “parkour” behavior revealed an innovative solution for particularly challenging leaps. Squirrels deciding and learning how to launch and land demonstrates the synergistic roles of biomechanics and cognition in

robust gap-crossing strategies.

Journal of Clinical Oncology (impact factor: 45.33) 1 

Global tissue stiffness on breast MR elastography: High-risk dense breast patients have higher stiffness compared to average-risk dense breast patients.

Bhavika K. Patel · Kay Pepin · Kathy R Brandt, et.al

Abstract

Background: Biomechanical tissue properties may vary in the breasts of patients at elevated risk for breast cancer. We aim to quantify in vivo biomechanical tissue properties in various breast densities and in both normal risk and high risk women using Magnetic Resonance Imaging (MRI)/MRE and examine the association of biomechanical properties of the breast with cancer risk. Methods: In this IRB-approved prospective single-institution study, we recruited two groups of women differing by breast cancer risk to undergo a 3.0 T dynamic contrast enhanced MRI/MRE of the breast. Low-average risk women were defined as having no personal or significant family history of breast cancer, no prior high risk breast biopsies and a negative mammography within 12 months. High-risk breast cancer patients were recruited from those patients who underwent standard of care breast MR. Within each breast density group (non-dense versus dense), two-sample t-tests were used to compare breast stiffness, elasticity, and viscosity across risk groups (low-average vs high). Results: There were 50 low-average risk and 86 high-risk patients recruited to the study. The risk groups were similar on age (mean age = 55.6 and 53.6 years), density (68% vs. 64% dense breasts) and menopausal status (66.0% vs. 69.8%). Among patients with dense breasts, mean stiffness, elasticity, and viscosity were significantly higher in high risk patients (N = 55) compared to low-average risk patients (N = 34; all $p < 0.001$). In the multivariate logistic regression model, breast stiffness remained a significant predictor of risk status (OR=4.26, 95% CI [1.96, 9.25]) even after controlling for breast density, MRI BPE, age, and menopausal status. Similar results were seen for breast elasticity (OR=4.88, 95% CI [2.08, 11.43]) and viscosity (OR=11.49, 95% CI [1.15, 114.89]). Conclusions: Structurally-based, quantitative biomarker of tissue stiffness obtained from global 3D breast MRE is associated with differences in breast cancer risk in dense breasts. As such, tissue stiffness could provide a novel prognostic marker to help identify the subset of high-risk women with dense breasts who would benefit from increased surveillance.

Computational Fluid Dynamics

Nature (impact factor: 64.84) 1 

Stabilization of liquid instabilities with ionized gas jets

Sanghoo Park · Wonho Choe · Hyungyu Lee, et.al

Abstract

Impinging gas jets can induce depressions in liquid surfaces, a phenomenon familiar to anyone who has observed the cavity produced by blowing air through a straw directly above a cup of juice. A dimple-like stable cavity on a liquid surface forms owing to the balance of forces among the gas jet impingement, gravity and surface tension^{1,2}. With increasing gas jet speed, the cavity becomes unstable and shows oscillatory motion, bubbling (Rayleigh instability) and splashing (Kelvin–Helmholtz instability)^{3,4}. However, despite its scientific and practical importance—particularly in regard to reducing cavity instability growth in certain gas-blown systems—little attention has been given to the hydrodynamic stability of a cavity in such gas–liquid systems so far. Here we demonstrate the stabilization of such instabilities by weakly ionized gas for the case of a gas jet impinging on water, based on shadowgraph experiments and computational two-phase fluid and plasma modelling. We focus on the interfacial dynamics relevant to electrohydrodynamic (EHD) gas flow, so-called electric wind, which is induced by the momentum transfer from accelerated charged particles to neutral gas under an electric field. A weakly ionized gas jet consisting of periodic pulsed ionization waves⁵, called plasma bullets, exerts more force via electrohydrodynamic flow on the water surface than a neutral gas jet alone, resulting in cavity expansion without destabilization. Furthermore, both the bidirectional electrohydrodynamic gas flow and electric field parallel to the gas–water interface produced by plasma interacting ‘in the cavity’ render the surface more stable. This case study demonstrates the dynamics of liquids subjected to a plasma-induced force, offering insights into physical processes and revealing an interdependence between weakly ionized gases and deformable dielectric matter, including plasma–liquid systems.

Progress in Energy and Combustion Science (impact factor: 29.54) 1 [X](#)


Transcritical diffuse-interface hydrodynamics of propellants in high-pressure combustors of chemical propulsion systems

Lluís Jofre · Javier Urzay

Abstract

Rocket engines and high-power new generations of gas-turbine jet engines and diesel engines oftentimes involve the injection of one or more reactants at subcritical temperatures into combustor environments at high pressures, and more particularly at pressures higher than those corresponding to the critical points of the individual components of the mixture, which typically range from 13 to 50 bars for most propellants. This class of trajectories in the thermodynamic space has been traditionally referred to as transcritical. However, the fundamental understanding of fuel atomization, vaporization, mixing, and combustion processes at such high pressures remains elusive. In particular, whereas fuel sprays are relatively well characterized at normal pressures, analyses of dispersion of fuel in high-pressure combustors are hindered by the limited experimental diagnostics and theoretical formulations available. The description of the

thermodynamics of hydrocarbon-fueled mixtures employed in chemical propulsion systems is complex and involves mixing-induced phenomena, including an elevation of the critical point whereby the coexistence region of the mixture extends up to pressures much larger than the critical pressures of the individual components. As a result, interfaces subject to surface-tension forces may persist in multicomponent systems despite the high pressures, and may give rise to unexpected spray-like atomization dynamics that are otherwise absent in monocomponent systems above their critical point. In this article, the current understanding of this phenomenon is reviewed within the context of propulsion systems fueled by heavy hydrocarbons. Emphasis is made on analytical descriptions at mesoscopic scales of interest for computational fluid dynamics. In particular, a set of modifications of the constitutive laws in the Navier–Stokes equations for multicomponent flows, supplemented with a high-pressure equation of state and appropriate redefinitions of the thermodynamic potentials, are introduced in this work based on an extended version of the diffuse-interface theory of van der Waals. The resulting formulation involves revisited forms of the stress tensor and transport fluxes of heat and species, and enables a description of the mesoscopic volumetric effects induced by transcritical interfaces consistently with the thermodynamic phase diagram of the mixture at high pressures. Applications of the theory are illustrated in canonical problems, including dodecane/nitrogen transcritical interfaces in non-isothermal systems. The results indicate that a transcritical interface is formed between the propellant streams that persists downstream of the injection orifice over distances of the same order as the characteristic thermal-entrance length of the fuel stream. The transcritical interface vanishes at an edge that gives rise to a fully supercritical mixing layer.

European Heart Journal (impact factor: 39.34) 1 

Long-term prognostic value of non-invasive lesion-specific hemodynamic index

S Y Yang · G C Choi · K L Lesina, et al

Abstract

Background

With advancement in computational fluid dynamics (CFD) technology, novel lesion-specific hemodynamic parameters can be estimated non-invasively. However, their long-term prognostic implications have not been fully defined.

Purpose

We sought to investigate the ten-year outcomes of lesion-specific hemodynamic indices derived-from coronary CT angiography (CCTA).

Methods

A total of 145 vessels (95 patients) with stable coronary artery disease who underwent fractional flow reserve (FFR) derived by coronary computed tomographic angiography (FFRCT) and invasive FFR measurement was included from the first-in-human study


of FFRCT. Study participants were enrolled from October 2009 to January 2011 and were followed up until December 2020. A total of 340 lesions with % diameter stenosis $\geq 30\%$ were identified, and wall shear stress (WSS) and change FFRCT across the lesion (Δ FFRCT) were obtained using CFD techniques by an independent core laboratory. The optimal cut-off for WSS and Δ FFRCT was applied for outcome analysis. The primary endpoint was target lesion failure (TLF) including cardiovascular death, target vessel myocardial infarction, and target lesion revascularization at 10 years.

Results

The median WSS and Δ FFRCT was 183.3 [112.8; 273.9] and 0.06 [0.03; 0.13]. WSS and Δ FFRCT was mildly correlated with FFRCT ($r=-0.18$, $P=0.001$ for WSS; $r=-0.36$, $P<0.001$ for Δ FFRCT). Of 179 lesions with deferral of revascularization at the index procedure of FFR measurement, TLF occurred in 16 (8.9%) lesions. In prediction of 10-year TLF, % diameter stenosis (per-lesion) $\geq 50\%$, FFRCT ≤ 0.80 , WSS ≥ 256.1 dyn/cm², and Δ FFRCT ≥ 0.06 were significant predictors. However, in multivariate analyses with those predictors, % diameter stenosis (per-lesion) $\geq 50\%$, FFRCT ≤ 0.80 became insignificant, and lesion-specific hemodynamic indices were only predictive of 10-year TLF (adjusted hazard ratio [aHR] 2.66, 95% confidence interval [CI] 0.98 - 7.22, $P=0.055$ for WSS ≥ 256.1 dyn/cm²; aHR 5.88, 95% CI 1.10 - 33.25, $P=0.045$ for Δ FFRCT ≥ 0.06). WSS ≥ 256.1 dyn/cm² and Δ FFRCT ≥ 0.06 had higher information gain in predicting outcomes than % diameter stenosis (per-lesion) $\geq 50\%$ and FFRCT ≤ 0.80 , and both improved predictability for 10-year TLF risk of the model with % diameter stenosis (per-lesion) $\geq 50\%$ and FFRCT ≤ 0.80 ($P=0.068$ for WSS ≥ 256.1 dyn/cm²; $P=0.011$ for Δ FFRCT ≥ 0.06) (Figure).

Conclusions

Non-invasive lesion-specific hemodynamic indices (i.e., high WSS and high Δ FFRCT) were the robust predictors of 10-year outcomes of a target lesion with incremental predictability over anatomical severity and low FFRCT. Clinical application of non-invasive hemodynamic indices will provide better long-term risk stratification over the current prognostication scheme before an invasive procedure.

European Heart Journal (impact factor: 39.34) 1 

Utilising clinical data to personalise boundary conditions significantly improves the accuracy of angiography based virtual FFR

R Gosling · E Gunn · H L Wei, et al

Abstract

Background

Angiography-derived computed (virtual) fractional flow reserve (vFFR) permits the assessment of coronary physiology without the need for a pressure wire or hyperaemia. However, accuracy is limited by assumptions made about coronary microvascular resistance (CMVR) [1]. We hypothesised that machine learning may allow us to “tune” our estimate of the CMVR to increase the accuracy of vFFR.

Purpose

To determine whether routine clinical data can personalise CMVR and improve the accuracy of vFFR on an individual case basis.

Methods


Patients with chronic coronary syndromes underwent coronary angiography with FFR assessment. Vessel-specific CMVR was computed using a 3D- computational fluid dynamics simulation with invasively measured proximal and distal pressures. Predictive models were created using non-linear autoregressing moving average with exogenous inputs (NARMAX) modelling with computed CMVR as the dependent variable. vFFR was computed using previously described methods [2]. Three simulations were run, using: 1) a generic CMVR value (Model A); 2) a NARMAX-predicted CMVR based upon a panel of simple clinical data (Model B); and 3) a NARMAX-predicted CMVR incorporating echocardiographic data (Model C). The diagnostic and quantitative accuracy of each model was compared with directly measured FFR.

Results

Eighty four patients underwent coronary angiography with FFR assessment in 157 vessels. Mean age was 64 (± 0.1) years and 64 (76%) were male. Mean FFR was 0.79 (± 0.15). Mean CMVR was 1.01×10^{10} Pa/m³ s⁻¹. vFFR error with Model A was ± 0.10 , with Model B was ± 0.07 ($p < 0.001$) and with Model C was ± 0.05 ($p < 0.001$) (Table 1).

Conclusion

vFFR is dependent upon not only the epicardial stenosis, but also the CMVR, estimation of which can be personalised based upon clinical and echocardiographic data. This can be used to increase the accuracy of vFFR.

European Heart Journal (impact factor: 39.34) 1 

Moving shear stress towards the clinic: preclinical comparison of optical coherence tomography-based versus angiography-based time-averaged wall shear stress estimations

J Naser · N Fogell · M Patel, et al

Abstract

Identification of coronary atherosclerotic plaques at risk of causing future acute coronary syndromes remains a major unmet clinical challenge. The addition of vessel biomechanics to intracoronary imaging derived evaluation of plaque morphology, improves identification of plaques likely to develop high risk features. We and others have developed a framework for intracoronary imaging (optical coherence tomography [OCT]) based 3D reconstructions of coronary arteries for computational fluid dynamics (CFD) simulations of shear stress, which are considered the current gold standard approach for quantification of coronary arterial haemodynamics. However, these approaches are time consuming and computationally intensive, resulting in a barrier to clinical uptake.

Purpose

Determination of time averaged wall shear stress (TAWSS) based on 3D coronary

geometries from non-invasive 3D Quantitative Coronary Angiography (3D-QCA) has recently been developed (Pie Medical Imaging, Netherlands), which enables results of shear stress simulations to be available within 30 minutes. We sought to compare TAWSS determined from 3D-QCA with gold standard OCT-based CFD simulations in both normal and stenotic arteries in minipigs.

Methods

15 normal and 5 stenotic minipig coronary arteries were studied. Anatomically matched 3D arterial geometries were reconstructed from 3D-QCA and OCT using common centrelines. Boundary conditions for simulations included directly measured inlet blood velocities; parabolic inlet flow profiles, zero pressure outlet; no-slip arterial walls; blood density: 1.05 g/ml; blood dynamic viscosity: 0.035 g/cm.s. Blood was modelled as Newtonian. 3D-QCA TAWSS was obtained with a Kratos Multi-Physics CFD solver. OCT-based simulations were performed using Abaqus/CFD v6.14. TAWSS was calculated for 80 axially matched segments for both methods (1200 and 400 paired comparisons for normal and stenotic arteries, respectively). Data were analysed using Bland-Altman and Wilcoxon matched-pairs signed ranked tests.


Results

Computation times for 3D-QCA and OCT-based CFD were approximately 30 minutes and 2 hours respectively. Axial profiles of TAWSS were similar between the two methods and there was agreement in TAWSS magnitudes and narrow 95% limits of agreement (Figure 1 and Figure 2). Using co-registered TAWSS maps generated by each method, we find similar spatial regional distributions of TAWSS in both normal and stenotic arteries.

Conclusions

Our data suggest that 3D-QCA based TAWSS is feasible in both normal and stenotic arteries. Spatial TAWSS distributions between the two methods are similar with agreement in matched TAWSS comparisons, though there are some small systematic differences in the absolute values of TAWSS, due to different resultant arterial geometries. These encouraging data suggest that further clinical evaluation of rapid TAWSS from 3D-QCA is warranted, which may facilitate clinical adoption of TAWSS assessment.

DESIGN AND MANUFACTURING

Science (impact factor: 56.91) 1 


The world of two-dimensional carbides and nitrides (MXenes)

Armin VahidMohammadi · Johanna Rosen · Yury Gogotsi

Abstract

A decade after the first report, the family of two-dimensional (2D) carbides and nitrides (MXenes) includes structures with three, five, seven, or nine layers of atoms

in an ordered or solid solution form. Dozens of MXene compositions have been produced, resulting in MXenes with mixed surface terminations. MXenes have shown useful and tunable electronic, optical, mechanical, and electrochemical properties, leading to applications ranging from optoelectronics, electromagnetic interference shielding, and wireless antennas to energy storage, catalysis, sensing, and medicine. Here we present a forward-looking review of the field of MXenes. We discuss the challenges to be addressed and outline research directions that will deepen the fundamental understanding of the properties of MXenes and enable their hybridization with other 2D materials in various emerging technologies.


Nature Reviews Materials (impact factor: 83.51) 1 

Lipid nanoparticles for mRNA delivery

Xucheng Hou · Tal Zaks · Robert Langer, et.al

Abstract:

Messenger RNA (mRNA) has emerged as a new category of therapeutic agent to prevent and treat various diseases. To function in vivo, mRNA requires safe, effective and stable delivery systems that protect the nucleic acid from degradation and that allow cellular uptake and mRNA release. Lipid nanoparticles have successfully entered the clinic for the delivery of mRNA; in particular, lipid nanoparticle–mRNA vaccines are now in clinical use against coronavirus disease 2019 (COVID-19), which marks a milestone for mRNA therapeutics. In this Review, we discuss the design of lipid nanoparticles for mRNA delivery and examine physiological barriers and possible administration routes for lipid nanoparticle–mRNA systems. We then consider key points for the clinical translation of lipid nanoparticle–mRNA formulations, including good manufacturing practice, stability, storage and safety, and highlight preclinical and clinical studies of lipid nanoparticle–mRNA therapeutics for infectious diseases, cancer and genetic disorders. Finally, we give an outlook to future possibilities and remaining challenges for this promising technology.

Lancet (impact factor:168.94) 1 


Urgent lessons from COVID 19: why the world needs a standing, coordinated system and sustainable financing for global research and development

Nicole Lurie · Gerald T Keusch · Victor J Dzau

Abstract:

The research and development (R&D) ecosystem has evolved over the past decade to include pandemic infectious diseases, building on experience from multiple recent outbreaks. Outcomes of this evolution have been particularly evident during the

COVID-19 pandemic with accelerated development of vaccines and monoclonal antibodies, as well as novel clinical trial designs. These products were developed, trialled, manufactured, and authorised for use in several countries within a year of the pandemic's onset. Many gaps remain, however, that must be bridged to establish a truly efficient and effective end-to-end R&D preparedness and response ecosystem. Foremost among them is a global financing system. In addition, important changes are required for multiple aspects of enabling sciences and product development. For each of these elements we identify priorities for improved and faster functionality. There will be no better time than now to seriously address these needs, however difficult, as the ravages of COVID-19 continue to accelerate with devastating health, social, and economic consequences for the entire community of nations.


Nature Energy (impact factor: 56.73) 1 

CO2 electrolysis to multicarbon products in strong acid

Fabian Duffner · Niklas Kronemeyer · Jens Tübke, et.al

Abstract:

Lithium-ion batteries are currently the most advanced electrochemical energy storage technology due to a favourable balance of performance and cost properties. Driven by forecasted growth of the electric vehicles market, the cell production capacity for this technology is continuously being scaled up. However, the demand for better performance, particularly higher energy densities and/or lower costs, has triggered research into post-lithium-ion technologies such as solid-state lithium metal, lithium–sulfur and lithium–air batteries as well as post-lithium technologies such as sodium-ion batteries. Currently, these technologies are being intensively studied with regard to material chemistry and cell design. In this Review, we expand on the current knowledge in this field. Starting with a market outlook and an analysis of technological differences, we discuss the manufacturing processes of these technologies. For each technology, we describe anode production, cathode production, cell assembly and conditioning. We then evaluate the manufacturing compatibility of each technology with the lithium-ion production infrastructure and discuss the implications for processing costs.

Science (impact factor: 56.91) 1 

Restoring metabolism of myeloid cells reverses cognitive decline in ageing

Dongdong Gu · Xinyu Shi · Reinhart Poprawe, et.al

Abstract:

Laser-metal additive manufacturing capabilities have advanced from single-material printing to multimaterial/multifunctional design and manufacturing. Material-structure-performance integrated additive manufacturing (MSPI-AM) represents a path toward

the integral manufacturing of end-use components with innovative structures and multimaterial layouts to meet the increasing demand from industries such as aviation, aerospace, automobile manufacturing, and energy production. We highlight two methodological ideas for MSPI-AM—“the right materials printed in the right positions” and “unique structures printed for unique functions”—to realize major improvements in performance and function. We establish how cross-scale mechanisms to coordinate nano/microscale material development, mesoscale process monitoring, and macroscale structure and performance control can be used proactively to achieve high performance with multifunctionality. MSPI-AM exemplifies the revolution of design and manufacturing strategies for AM and its technological enhancement and sustainable development.

II Concentration

PHYSICS

Continuous and efficient elastocaloric air cooling by coil-bending

Li, Xueshi, Hua, Peng, , et al.

Abstract

Elastocaloric cooling has emerged as an eco-friendly technology capable of eliminating greenhouse-gas refrigerants. However, its development is limited by the large driving force and low efficiency in uniaxial loading modes. Here, we present a low-force and energy-efficient elastocaloric air cooling approach based on coil-bending of NiTi ribbons/wires. Our air cooler achieves continuous cold outlet air with a temperature drop of 10.6 K and a specific cooling power of 2.5 W g⁻¹ at a low specific driving force of 26 N g⁻¹. Notably, the cooler shows a system coefficient of performance of 3.7 (ratio of cooling power to rotational mechanical power). These values are realized by the large specific heat transfer area (12.6 cm² g⁻¹) and the constant cold zone of NiTi wires. Our coil-bending system exhibits a competitive performance among caloric air coolers.

Telecom-band quantum dot technologies for long-distance quantum networks

Yu, Ying, Liu, et al.

Abstract

A future quantum internet is expected to generate, distribute, store and process quantum bits (qubits) over the world by linking different quantum nodes via quantum states of light. To facilitate long-haul operations, quantum repeaters must operate at telecom wavelengths to take advantage of both the low-loss optical fibre network and the established technologies of modern optical communications. Semiconductor quantum dots have thus far shown exceptional performance as key elements for quantum repeaters, such as quantum light sources and spin-photon interfaces, but only in the near-infrared regime. Therefore, the development of high-performance telecom-band quantum dot devices is highly desirable for a future solid-state quantum internet based on fibre networks. In this Review, we present the physics and technological developments towards epitaxial quantum dot devices emitting in the telecom O- and C-bands for quantum networks, considering both advanced epitaxial growth for direct telecom emission and quantum frequency conversion for telecom-band down-

conversion of near-infrared quantum dot devices. We also discuss the challenges and opportunities for future realization of telecom quantum dot devices with improved performance and expanded functionality through hybrid integration.

Ultraviolet interlayer excitons in bilayer WSe₂

Lin, Kai-Qiang, Faria Junior, et al.

Abstract

Interlayer excitons in van der Waals heterostructures are fascinating for applications like exciton condensation, excitonic devices and moiré-induced quantum emitters. The study of these charge-transfer states has almost exclusively focused on band edges, limiting the spectral region to the near-infrared regime. Here we explore the above-gap analogues of interlayer excitons in bilayer WSe₂ and identify both neutral and charged species emitting in the ultraviolet. Even though the transitions occur far above the band edge, the states remain metastable, exhibiting linewidths as narrow as 1.8 meV. These interlayer high-lying excitations have switchable dipole orientations and hence show prominent Stark splitting. The positive and negative interlayer high-lying trions exhibit significant binding energies of 20–30 meV, allowing for a broad tunability of transitions via electric fields and electrostatic doping. The Stark splitting of these trions serves as a highly accurate, built-in sensor for measuring interlayer electric field strengths, which are exceedingly difficult to quantify otherwise. Such excitonic complexes are further sensitive to the interlayer twist angle and offer opportunities to explore emergent moiré physics under electrical control. Our findings more than double the accessible energy range for applications based on interlayer excitons.

MATERIALS

Self-enhancing sono-inks enable deep-penetration acoustic volumetric printing

Xiao Kuang, Qiangzhou Rong, Saud Belal, et al.

Abstract

Volumetric printing, an emerging additive manufacturing technique, builds objects with enhanced printing speed and surface quality by forgoing the stepwise ink-renewal step. Existing volumetric printing techniques almost exclusively rely on light energy to trigger photopolymerization in transparent inks, limiting material choices and build sizes. We report a self-enhancing sonicated ink (or sono-ink) design and corresponding focused-ultrasound writing technique for deep-penetration acoustic volumetric printing (DAVP). We used experiments and acoustic modeling to study the frequency and scanning rate-dependent acoustic printing behaviors. DAVP achieves the key features

of low acoustic streaming, rapid sonothermal polymerization, and large printing depth, enabling the printing of volumetric hydrogels and nanocomposites with various shapes regardless of their optical properties. DAVP also allows printing at centimeter depths through biological tissues, paving the way toward minimally invasive medicine.

Lateral epitaxial growth of two-dimensional organic heterostructures

lv, Qiang, Wang, et al.

Abstract

Two-dimensional organic lateral heterostructures (2D OLHs) are attractive for the fabrication of functional materials. However, it is difficult to control the nucleation, growth and orientation of two distinct components. Here we report the combination of two methods—liquid-phase growth and vapour-phase growth—to synthesize 2D OLHs from perylene and a perylenecarboxaldehyde derivative, with a lateral size of $\sim 20\ \mu\text{m}$ and a tunable thickness ranging from 20 to 400 nm. The screw dislocation growth behaviour of the 2D crystals shows the spiral arrangement of atoms within the crystal lattice, which avoids volume expansion and contraction of OLH, thereby minimizing lateral connection defects. Selective control of the nucleation and sequential growth of 2D crystals leads to structural inversion of the 2D OLHs by the vapour-phase growth method. The resulting OLHs show good light-transport capabilities and tunable spatial exciton conversion, useful for photonic applications. This synthetic strategy can be extended to other families of organic polycyclic aromatic hydrocarbons, as demonstrated with other pyrene and perylene derivatives.

A stable atmospheric-pressure plasma for extreme-temperature synthesis

Xie, Hua, Liu, et al.

Abstract

Plasmas can generate ultra-high-temperature reactive environments that can be used for the synthesis and processing of a wide range of materials^{1,2}. However, the limited volume, instability and non-uniformity of plasmas have made it challenging to scalably manufacture bulk, high-temperature materials^{3,4,5,6,7,8}. Here we present a plasma set-up consisting of a pair of carbon-fibre-tip-enhanced electrodes that enable the generation of a uniform, ultra-high temperature and stable plasma (up to 8,000 K) at atmospheric pressure using a combination of vertically oriented long and short carbon fibres. The long carbon fibres initiate the plasma by micro-spark discharge at a low breakdown voltage, whereas the short carbon fibres coalesce the discharge into a volumetric and stable ultra-high-temperature plasma. As a proof of concept, we used this process to synthesize various extreme materials in seconds, including ultra-high-temperature ceramics (for example, hafnium carbonitride) and refractory metal alloys.

Moreover, the carbon-fibre electrodes are highly flexible and can be shaped for various syntheses. This simple and practical plasma technology may help overcome the challenges in high-temperature synthesis and enable large-scale electrified plasma manufacturing powered by renewable electricity.

CHEMISTRY

Efficient multicarbon formation in acidic CO₂ reduction via tandem electrocatalysis

Chen, Yuanjun, Li, et al.

Abstract

The electrochemical reduction of CO₂ in acidic conditions enables high single-pass carbon efficiency. However, the competing hydrogen evolution reaction reduces selectivity in the electrochemical reduction of CO₂, a reaction in which the formation of CO, and its ensuing coupling, are each essential to achieving multicarbon (C₂⁺) product formation. These two reactions rely on distinct catalyst properties that are difficult to achieve in a single catalyst. Here we report decoupling the CO₂-to-C₂⁺ reaction into two steps, CO₂-to-CO and CO-to-C₂⁺, by deploying two distinct catalyst layers operating in tandem to achieve the desired transformation. The first catalyst, atomically dispersed cobalt phthalocyanine, reduces CO₂ to CO with high selectivity. This process increases local CO availability to enhance the C–C coupling step implemented on the second catalyst layer, which is a Cu nanocatalyst with a Cu–ionomer interface. The optimized tandem electrodes achieve 61% C₂H₄ Faradaic efficiency and 82% C₂⁺ Faradaic efficiency at 800 mA cm⁻² at 25 °C. When optimized for single-pass utilization, the system reaches a single-pass carbon efficiency of 90 ± 3%, simultaneous with 55 ± 3% C₂H₄ Faradaic efficiency and a total C₂⁺ Faradaic efficiency of 76 ± 2%, at 800 mA cm⁻² with a CO₂ flow rate of 2 ml min⁻¹.

A general copper-catalysed enantioconvergent C(sp³)-S cross-coupling via biomimetic radical homolytic substitution

Tian, Yu, Li, et al.

Abstract

Although α -chiral C(sp³)-S bonds are of enormous importance in organic synthesis and related areas, the transition-metal-catalysed enantioselective C(sp³)-S bond construction still represents an underdeveloped domain probably due to the difficult

heterolytic metal–sulfur bond cleavage and notorious catalyst-poisoning capability of sulfur nucleophiles. Here we demonstrate the use of chiral tridentate anionic ligands in combination with Cu(I) catalysts to enable a biomimetic enantioconvergent radical C(sp³)–S cross-coupling reaction of both racemic secondary and tertiary alkyl halides with highly transformable sulfur nucleophiles. This protocol not only exhibits a broad substrate scope with high enantioselectivity but also provides universal access to a range of useful α -chiral alkyl organosulfur compounds with different sulfur oxidation states, thus providing a complementary approach to known asymmetric C(sp³)–S bond formation methods. Mechanistic results support a biomimetic radical homolytic substitution pathway for the critical C(sp³)–S bond formation step.

On-surface synthesis of aromatic cyclo[10]carbon and cyclo[14]carbon

Sun, Luye, Zheng, et al.

Abstract

All-carbon materials based on sp²-hybridized atoms, such as fullerenes¹, carbon nanotubes² and graphene³, have been much explored due to their remarkable physicochemical properties and potential for applications. Another unusual all-carbon allotrope family are the cyclo[n]carbons (C_n) consisting of two-coordinated sp²-hybridized atoms. They have been studied in the gas phase since the twentieth century^{4,5,6}, but their high reactivity has meant that condensed-phase synthesis and real-space characterization have been challenging, leaving their exact molecular structure open to debate^{7,8,9,10,11}. Only in 2019 was an isolated C₁₈ generated on a surface and its polyynic structure revealed by bond-resolved atomic force microscopy^{12,13}, followed by a recent report¹⁴ on C₁₆. The C₁₈ work triggered theoretical studies clarifying the structure of cyclo[n]carbons up to C₁₀₀ (refs. 15,16,17,18,19,20), although the synthesis and characterization of smaller C_n allotropes remains difficult. Here we modify the earlier on-surface synthesis approach to produce cyclo[10]carbon (C₁₀) and cyclo[14]carbon (C₁₄) via tip-induced dehalogenation and retro-Bergman ring opening of fully chlorinated naphthalene (C₁₀Cl₈) and anthracene (C₁₄Cl₁₀) molecules, respectively. We use atomic force microscopy imaging and theoretical calculations to show that, in contrast to C₁₈ and C₁₆, C₁₀ and C₁₄ have a cumulenic and cumulene-like structure, respectively. Our results demonstrate an alternative strategy to generate cyclocarbons on the surface, providing an avenue for characterizing annular carbon allotropes for structure and stability.

BIOLOGY

Single-cell CRISPR screens in vivo map T cell fate regulomes in cancer

Zhou, Peipei, Shi, et al.

Abstract

CD8⁺ cytotoxic T cells (CTLs) orchestrate antitumour immunity and exhibit inherent heterogeneity^{1,2}, with precursor exhausted T (Tpex) cells but not terminally exhausted T (Tex) cells capable of responding to existing immunotherapies^{3,4,5,6,7}. The gene regulatory network that underlies CTL differentiation and whether Tex cell responses can be functionally reinvigorated are incompletely understood. Here we systematically mapped causal gene regulatory networks using single-cell CRISPR screens in vivo and discovered checkpoints for CTL differentiation. First, the exit from quiescence of Tpex cells initiated successive differentiation into intermediate Tex cells. This process is differentially regulated by IKAROS and ETS1, the deficiencies of which dampened and increased mTORC1-associated metabolic activities, respectively. IKAROS-deficient cells accumulated as a metabolically quiescent Tpex cell population with limited differentiation potential following immune checkpoint blockade (ICB). Conversely, targeting ETS1 improved antitumour immunity and ICB efficacy by boosting differentiation of Tpex to intermediate Tex cells and metabolic rewiring. Mechanistically, TCF-1 and BATF are the targets for IKAROS and ETS1, respectively. Second, the RBPJ–IRF1 axis promoted differentiation of intermediate Tex to terminal Tex cells. Accordingly, targeting RBPJ enhanced functional and epigenetic reprogramming of Tex cells towards the proliferative state and improved therapeutic effects and ICB efficacy. Collectively, our study reveals that promoting the exit from quiescence of Tpex cells and enriching the proliferative Tex cell state act as key modalities for antitumour effects and provides a systemic framework to integrate cell fate regulomes and reprogrammable functional determinants for cancer immunity.

iPS-cell-derived microglia promote brain organoid maturation via cholesterol transfer

Park, Dong Shin, Kozaki, et al.

Abstract

Microglia are specialized brain-resident macrophages that arise from primitive macrophages colonizing the embryonic brain¹. Microglia contribute to multiple aspects of brain development, but their precise roles in the early human brain remain poorly understood owing to limited access to relevant tissues^{2,3,4,5,6}. The generation of brain organoids from human induced pluripotent stem cells recapitulates some key features of human embryonic brain development^{7,8,9,10}. However, current approaches do not incorporate microglia or address their role in organoid maturation^{11,12,13,14,15,16,17,18,19,20,21}. Here we generated microglia-sufficient brain organoids by coculturing brain organoids with primitive-like macrophages

generated from the same human induced pluripotent stem cells (iMac)²². In organoid cocultures, iMac differentiated into cells with microglia-like phenotypes and functions (iMicro) and modulated neuronal progenitor cell (NPC) differentiation, limiting NPC proliferation and promoting axonogenesis. Mechanistically, iMicro contained high levels of PLIN2⁺ lipid droplets that exported cholesterol and its esters, which were taken up by NPCs in the organoids. We also detected PLIN2⁺ lipid droplet-loaded microglia in mouse and human embryonic brains. Overall, our approach substantially advances current human brain organoid approaches by incorporating microglial cells, as illustrated by the discovery of a key pathway of lipid-mediated crosstalk between microglia and NPCs that leads to improved neurogenesis.

Organ aging signatures in the plasma proteome track health and disease

Oh, Hamilton Se-Hwee, Rutledge, et al.

Abstract

Animal studies show aging varies between individuals as well as between organs within an individual^{1,2,3,4}, but whether this is true in humans and its effect on age-related diseases is unknown. We utilized levels of human blood plasma proteins originating from specific organs to measure organ-specific aging differences in living individuals. Using machine learning models, we analysed aging in 11 major organs and estimated organ age reproducibly in five independent cohorts encompassing 5,676 adults across the human lifespan. We discovered nearly 20% of the population show strongly accelerated age in one organ and 1.7% are multi-organ agers. Accelerated organ aging confers 20–50% higher mortality risk, and organ-specific diseases relate to faster aging of those organs. We find individuals with accelerated heart aging have a 250% increased heart failure risk and accelerated brain and vascular aging predict Alzheimer's disease (AD) progression independently from and as strongly as plasma pTau-181 (ref. 5), the current best blood-based biomarker for AD. Our models link vascular calcification, extracellular matrix alterations and synaptic protein shedding to early cognitive decline. We introduce a simple and interpretable method to study organ aging using plasma proteomics data, predicting diseases and aging effects.

III Calling for papers

ACAE 2024

Submission deadline:	Dec 20, 2023
Conference date:	May 8, 2024 - May 10, 2024
Full name:	2024 the 5th Asia Conference on Automation Engineering (ACAE 2024)
Location:	Melbourne, Australia
Website:	http://www.acae.net/

Publication

The accepted papers after registration will be published into ACAE 2024 conference proceedings. It will be published online, and will be submitted for indexing by Ei Compendex, Scopus.

Submission

1. Full Paper (Publication and Presentation)
2. Abstract (Presentation Only)

Electronic Submission System: <https://www.zmeeting.org/submission/acae2024>

Any question, please contact: acae@academic.net

More details about submission, please visit at <http://acae.net/sub.html>

Conference Schedule

May 8th, 2024 | Sign in and Collect Conference Materials

May 9th, 2024 | Welcome Messages & Keynote Speeches/ Parallel Sessions for Authors' Presentations

May 10th, 2024 | One Day Visit / Academic Visit (pending)

Conference Venue

Royal Melbourne Institute of Technology, Australia

Venue: 124 La Trobe St, Melbourne VIC

Contact Us

Ms. Lorraine Lee (Conference Secretary)

Email: acae@academic.net

Tel: +001(559)-8624927 / +86-18117807842

(Office Time 9:30 - 18:00, Time zone: GMT+8; Monday to Friday)

Topics include, but not limited to:

- adaptive automation systems
- Agent-based collaborative automation systems
- Application design
- Automated fault detection, diagnostics, and prognostics
- Automation in life science
- Autonomous systems
- Big data, data mining, and machine learning
- Cloud-based automation
- Cognitive Automation
- ...

ICMENS 2024

Submission deadline:	Dec 21, 2023
Conference date:	Mar 22, 2024 - Mar 25, 2024
Full name:	2024 8th International Conference on Materials Engineering and Nano Sciences (ICMENS 2024)
Location:	Osaka, Japan
Website:	http://www.icmens.org

2024 8th International Conference on Materials Engineering and Nano Sciences (ICMENS 2024) will be held in Kwansai Gakuin University, Osaka, Japan during March 22-25, 2024. The conference is co-sponsored by Kwansai Gakuin University, Japan and Chiba University, Japan.

Materials Engineering based on Nano Sciences is a key ingredient of current advanced technologies supporting modern society, especially Information and Energy Technologies. The tremendous rapid growth of these fields makes them highly interdisciplinary and then inevitably demands their mutual interactions. Under these circumstances, the 2024 8th International Conference on Materials Engineering and Nano Sciences (ICMENS 2024) was organized as a series of successful international conferences held in Singapore (2017), Hong Kong (2018), Hiroshima (2019, Japan), Pattaya (2020, Thailand), Online (2021&2022), and Chiba University (2023, Japan).

The main goal of ICMENS is to address latest original results in Materials Engineering and Nano Sciences, including both theoretical advances and practical implementations, which are becoming more and more popular in industry and in our daily lives. ICMENS will provide a premier interdisciplinary platform for scientists, researchers, industry leaders, engineers and educators throughout the world to present and discuss the most recent innovations, trends, concerns, as well as practical challenges encountered, and streamline solutions in the fields of Materials Engineering and Nano Sciences. The meeting will provide an opportunity to highlight recent developments and to identify emerging and future areas of growth in Quantum Technology.

The organizing committee of conference is pleased to invite prospective authors to submit their original manuscripts to ICMENS 2024.

Topics:

1. Materials Engineering
Advanced Characterization
Biological Materials
Materials for Energy and Environmental Applications
Biotechnology and Life Sciences
Materials Processing
Mechanical Behavior of Materials
Computational Materials Science
Mechanical Properties and Nanomechanics
Nanotechnology

Optical and Photonic Materials
Economics of Materials
Optoelectronics
Electrochemistry
2. Nano Sciences
Nanotechnology and Materials Sciences
Nanooptics and Nanophotonics
Materials Science and Engineering: Nanotechnology
Nanowires
Advanced Applications in Nanoscience and Nanotechnology
Nanofluidics
Carbon Nanotubes and Biomolecules
Nanobiotechnology
Nanomaterials
Nanoscale Science and Technology

ICMES 2024

Submission deadline: Jan 1, 2024
Conference date: May 14, 2024 - May 16, 2024
Full name: 2024 the 9th International Conference on Mechatronics and Electrical Systems (ICMES 2024)
Location: Shenzhen, China
Website: <http://www.icmes.org/>

2024 the 9th International Conference on Mechatronics and Electrical Systems (ICMES 2024) will be held in Shenzhen, China from May 14-16, 2024, held together with ICACR 2024. It sponsored by Southern University of Science and Technology (SUSTech). On behalf of the conference committees, it is our pleasure and honor to invite prospective authors initiating the discussion on the challenges that need to be timely overcome and addressing key questions for achieving a safe, reliable, sustainable and intelligent power system.

Topics:

- Advances in Aerospace and Automotive
- Agrotechnology
- Applied Sciences and Biosciences
- Biomechanics and Medical Technology
- Electrical and Electronic System
- Control, Robotics And Mechatronics
- Artificial Intelligence and Intelligent Control
- Social Science Studies Related to Engineering and Technology
- Mechatronics Applications in Cyber-physical Systems
- Diagnosis and Monitoring in Mechatronic Systems
- Strategic and Defence Technology
- Structural and Environment Engineering
- Transportation Systems
- Tribology

ICAMM--SCOPUS 2024

Submission deadline: Feb 23, 2024
Conference date: Jul 10, 2024 - Jul 12, 2024
Full name: 2024 8th International Conference on Advanced Manufacturing and Materials (ICAMM 2024)
Location: Edinburgh, United Kingdom
Website: <http://www.icamm.org>

2024 8th International Conference on Advanced Manufacturing and Materials (ICAMM 2024), will be held in Edinburgh, United Kingdom during July 10-12, 2024.

ICAMM 2024 is organized after ICAMM 2023 held in Cambridge, ICAMM 2022 & ICAMM 2021 & ICAMM 2020 held virtually, ICAMM 2019 held in Beihang University, Beijing, China. ICAMM 2018 held in Tokyo, Japan during June 11-13, 2018. ICAMM 2017 held in The Hong Kong Polytechnic University, Hong Kong during June 25-27, 2017. ICAMM focuses on the advanced manufacturing and materials research. The applications of advanced manufacturing and materials to such domains as Multi-scale and/or Multi-disciplinary Approaches, Chemistry and Chemical Engineering Fundamentals et al. It is a technical congregation where the latest theoretical and technological advances are presented and discussed.

Topics of interest for submission include, but are not limited to:

- Materials
 - Composite Materials
 - New Materials
 - Materials Properties, Measuring Methods and Applications
 - Superconducting Materials and technology
 - Nanotechnology, Nano-Materials and Nano-Composites

- Manufacturing
 - Materials Manufacturing and Processing
 - Casting, Powder Metallurgy
 - Welding, Sintering, Heat Treatment
 - Thin & Thick Coatings
 - Surface Treatment, Machining

*More topics, please go to: <http://www.icamm.org/cfp.html>